

Ring cavity fiber laser based on Fabry-Pérot interferometer for high-sensitive micro-displacement sensing*

BAI Yan (白燕), YAN Feng-ping (延凤平)**, LIU Shuo (刘硕), TAN Si-yu (谭思宇), and WEN Xiao-dong (温晓东)

Key Laboratory of All Optical Network & Advanced Telecommunication Network, Education Ministry of China, Beijing Jiaotong University, Beijing 100044, China

(Received 5 August 2015)

©Tianjin University of Technology and Springer-Verlag Berlin Heidelberg 2015

A ring cavity fiber laser based on Fabry-Pérot interferometer (FPI) is proposed and demonstrated experimentally for micro-displacement sensing. Simulation results show that the dips of the FPI transmission spectrum are sensitive to the cavity length of the FPI. With this characteristic, the relationship between wavelength shift and cavity length change can be established by means of the FPI with two aligned fiber end tips. The maximum sensitivity of 39.6 nm/ μm is achieved experimentally, which is approximately 25 times higher than those in previous reports. The corresponding ring cavity fiber laser with the sensitivity for displacement measurement of about 6 nm/ μm is implemented by applying the FPI as the filter. The proposed fiber laser has the advantages of simple structure, low cost and high sensitivity.

Document code: A **Article ID:** 1673-1905(2015)06-0421-5

DOI 10.1007/s11801-015-5152-5

Fiber laser sensors are capable of detecting liquid/gas refractive index, temperature, strain/stress, humidity, displacement/distance, curvature, and so on. Among them, the displacement fiber sensors play important roles in modern industrial processes especially. Many fiber sensors based on wavelength shift have been investigated, including fiber gratings, fiber interferometers as well as the combination of them. Fiber Bragg grating (FBG)^[1-5] and tilted fiber Bragg grating (TFBG)^[6] are the typical grating structures for displacement sensing. Comparatively speaking, most fiber interferometers are easy to fabricate and low in price, and their sensitivities are usually higher for lots of parameters measurement. These fiber interferometers include many types of structures, such as Mach-Zehnder interferometer (MZI)^[7,8], Michelson interferometer^[9,10], Sagnac interferometer (SI)^[11] and Fabry-Pérot interferometer (FPI)^[12,13]. All of these interferometers have the capacity to detect displacement. Particularly, SI and FPI are more stable to the ambient temperature fluctuation and vibration due to their single fiber ring structure. The fiber FPI is usually composed of two aligned mirrors with a certain distance between them, and any additional special optical fiber is not necessary. Moreover, the FPI has high sensitivity to many ambient parameters, such as temperature and displacement.

In this paper, a ring cavity fiber laser based on the all fiber FPI is proposed and demonstrated experimentally for micro-displacement measurement. The FPI is com-

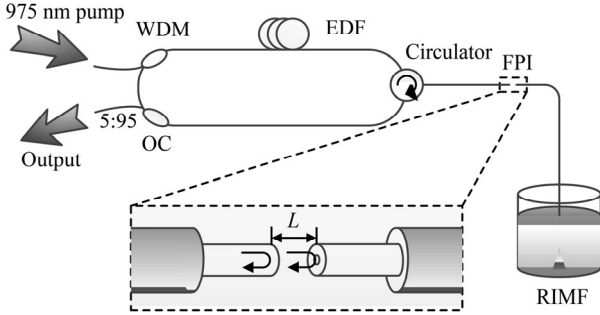
posed of two fiber ends with a gap between them. The distance between the two fiber end faces can influence the transmission spectrum of the FPI, and thus this kind of FPI can be applied to detect the displacement. The maximum sensitivity of 39.6 nm/ μm , which is much higher than that in Ref.[14], is achieved experimentally. The experimental results show that for this system, there is an approximately linear relationship between wavelength and displacement with sensitivity of 6 nm/ μm which is about four times of 1.533 nm/ μm achieved by the previous MZI^[14].

A ring cavity fiber laser with the filter based on FPI is used for high-sensitive micro-displacement sensing, and the schematic diagram is shown in Fig.1. The laser diode with central wavelength of 975 nm provides the pump power which is coupled into the ring cavity by a wavelength division multiplexer (WDM, 1550/975). The erbium doped fiber (EDF) serves as the gain medium. A 5:95 fiber coupler is connected to the optical spectrum analyzer (OSA) for signal detection. The circulator in the fiber ring can not only force the optical signal to transmit along a single direction, but also connect the FPI to the ring cavity. The inset in Fig.1 shows the schematic diagram of the FPI, where L indicates the length of the Fabry-Pérot cavity (FPC). Refractive index matching fluid is applied for absorbing the useless light from the pigtail of the FPI. The transmission spectrum of the FPI is related to the length of FPC. In other words, the filter

* This work has been supported by the National Natural Science Foundation of China (Nos.61275091 and 61327006).

** E-mail: fpyan@bjtu.edu.cn

based on FPI is sensitive to the relative position of the two fiber ends, so that it can be applied for displacement sensing.



WDM: wavelength division multiplexer; EDF: erbium doped fiber; FPI: Fabry-Pérot interferometer; OC: optical coupler; POJ: point of junction; RIMF: refractive index matching fluid

Fig.1 Schematic diagram of the proposed laser sensing system (The inset is the schematic diagram of the fiber Fabry-Pérot interferometer, where L is the cavity length of the FPI.)

This type of FPI is composed of the end faces of two aligned fibers, and the distance (L) determines the cavity length of the FPI. The light will be reflected by the end faces of two fibers. However, Fresnel reflection of the fiber end faces can only provide the reflectivity of 4%, and thus the intensities of the light paths with multiple reflections are so weak that they can be ignored. As a result, two main paths of light are taken into account in the numerical simulation, and the transmission spectrum of the proposed FPI can be expressed as

$$I = I_1 + I_2 + 2\sqrt{I_1 I_2} \cos(\Delta\delta), \quad (1)$$

where I_1 and I_2 are the intensities of the two paths of light, respectively. Firstly, one path of light (I_1) is reflected by the left fiber end. Secondly, the other one (I_2) transmits through the left fiber end, and then it is reflected by the right fiber end. Finally, the latter path of light goes through the left fiber end, and interferes with the former one afterwards. $\Delta\delta$ is the phase difference of the two paths of light^[15], and it can be expressed as

$$\Delta\delta = \frac{2\pi}{\lambda} \cdot 2n_{\text{air}}L, \quad (2)$$

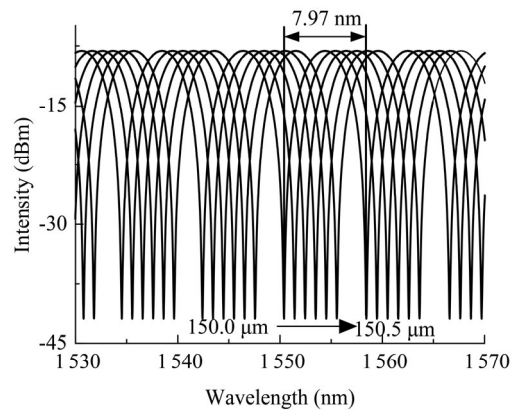
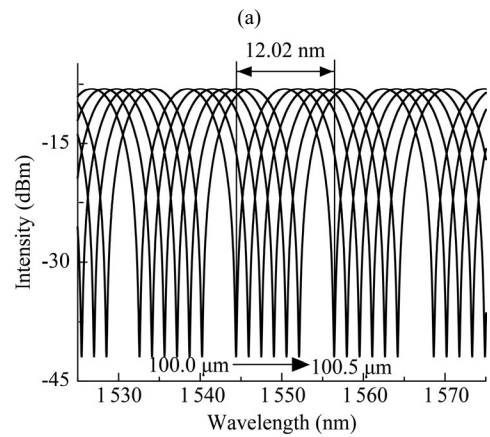
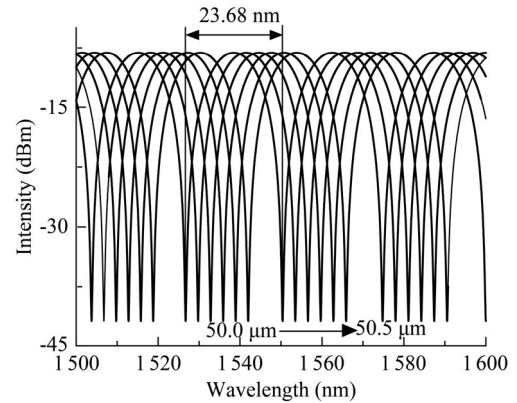
where n_{air} indicates the refractive index of air and can be deemed as a constant, λ is the wavelength in vacuum, and L is the length of the FPC. From Eqs.(1) and (2), it can be seen that the transmission spectrum intensity I is related to the length of FPC, which is the displacement sensing principle of the proposed FPI.

All the dips move to the long wavelength direction with the increase of L as shown in Fig.2. In addition, the fringe spacing (FS) drops down with the increase of

original L by comparing Fig.2(a)–(d), which is coincident with the previous theoretical derivation as^[16,17]

$$FS = \frac{\lambda^2}{n_{\text{eff}} \cdot 2L}, \quad (3)$$

where n_{eff} is the effective index of the air and can be approximate to be $n_{\text{eff}}=1$. When λ is set to be a certain value, there is an inversely proportional relationship between the FS and the length of the FPC. The wavelength shifts of the dips with various displacements can be achieved as shown in Fig.3(a), and Fig.3(b) shows the sensitivities of the FPI for displacement sensing. It can be seen that the smaller the original L , the higher the sensitivity of the FPI.



(c)

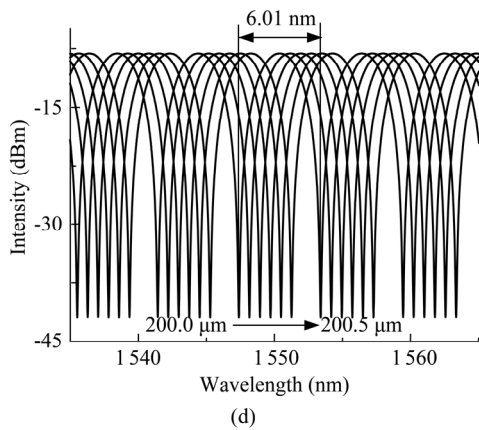


Fig.2 The transmission spectra of the FPI with various lengths of the FPC of (a) $L=50.0-50.5 \mu\text{m}$, (b) $L=100.0-100.5 \mu\text{m}$, (c) $L=150.0-150.5 \mu\text{m}$ and (d) $L=200.0-200.5 \mu\text{m}$ with interval of $0.1 \mu\text{m}$

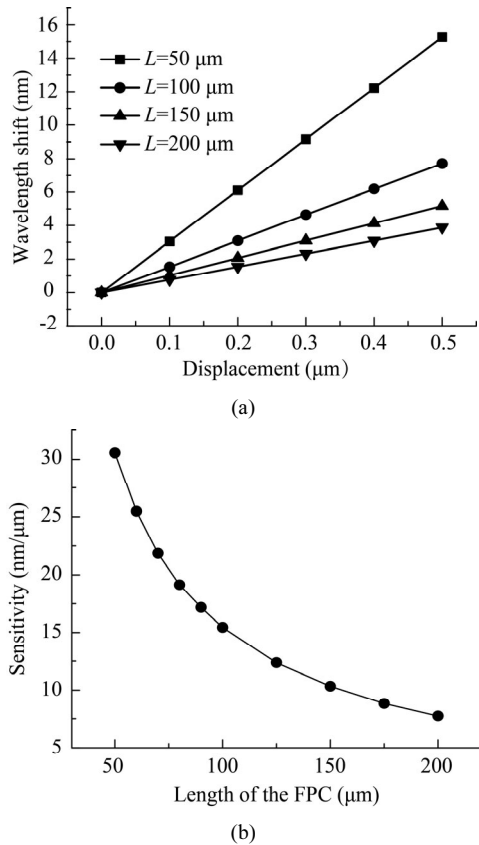


Fig.3 (a) Wavelength shift as a function of the displacement with different original L ; (b) Sensitivities of the FPI with various lengths of the FPC

Since the FPI is the filter in a ring cavity laser, its cavity length should be set as a suitable value so that there is only one visible and stable peak in the whole detecting wavelength range. Overlarge FS will introduce instable peak fluctuation, and multiple peaks can be generated when the FS is too small. Meanwhile, the measurable displacement range of the proposed laser declines with a larger original L , because another peak in the wavelength

ranges of adjacent FS will be stimulated when the peak shifts across the boundary value of the FS.

The transmission spectrum of the FPI can be measured by the means of the setup shown in Fig.4. The broadband source (BBS, KOHERAS, superK uersa) is used to provide the broadband light, and the OSA (YOKOGAWA, AQ6375) is used to detect the spectrum. By applying various lengths of the FPC, four spectra are achieved as shown in Fig.5. It can be clearly seen that the dips of all the curves move to the long wavelength direction with the increase of L , and the values of the wavelength shift in Fig.5(a) are much larger than those in Fig.5(b)–(d). In other words, the wavelength shift is related to the original L . Fig.6 shows the good linear relationships between wavelength shift of the peak and the displacement with the original $L=40 \mu\text{m}$, $108 \mu\text{m}$, $165 \mu\text{m}$ and $223 \mu\text{m}$, respectively. As shown in Fig.6, a smaller original L will cause a larger sensitivity.

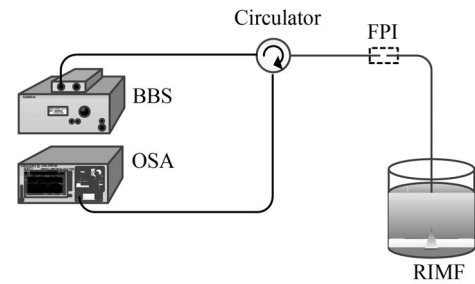
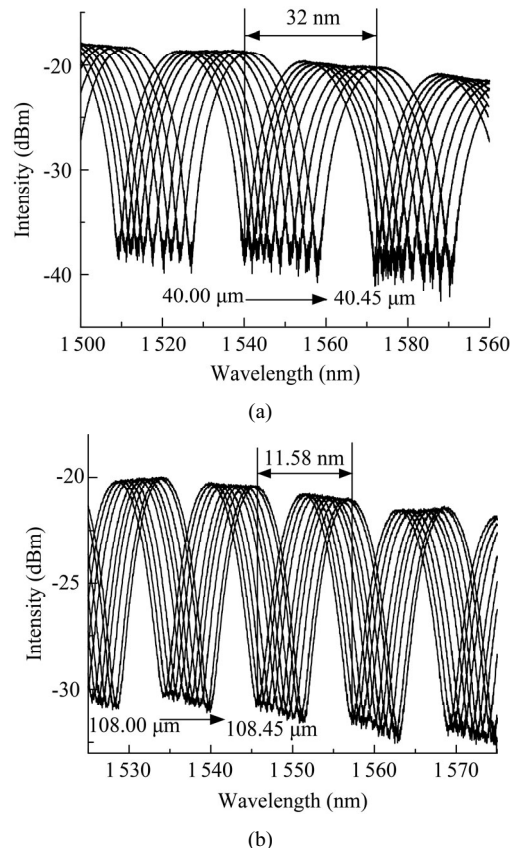


Fig.4 Schematic diagram of the setup for the measurement of the FPI transmission spectrum



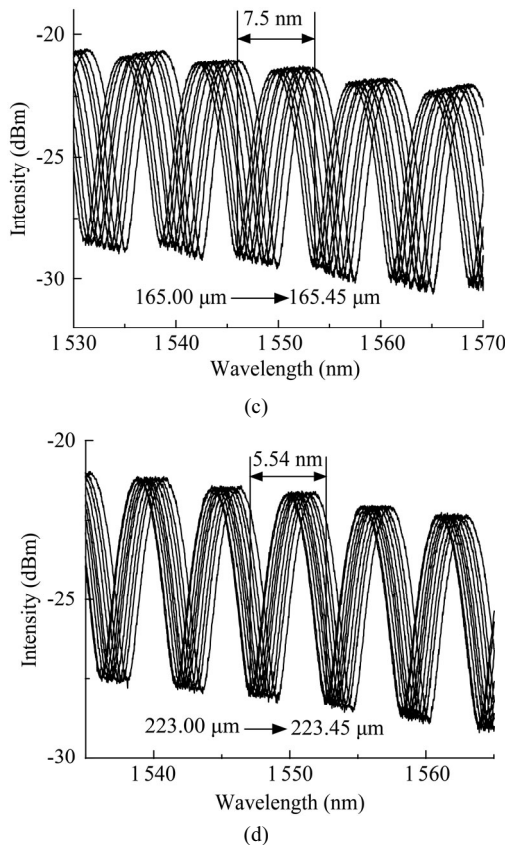


Fig.5 The transmission spectra of the FPI with various lengths of the FPC of (a) $L=40.00\text{--}40.45\ \mu\text{m}$, (b) $L=108.00\text{--}108.45\ \mu\text{m}$, (c) $L=165.00\text{--}165.45\ \mu\text{m}$ and (d) $L=223.00\text{--}223.45\ \mu\text{m}$ with interval of $0.05\ \mu\text{m}$

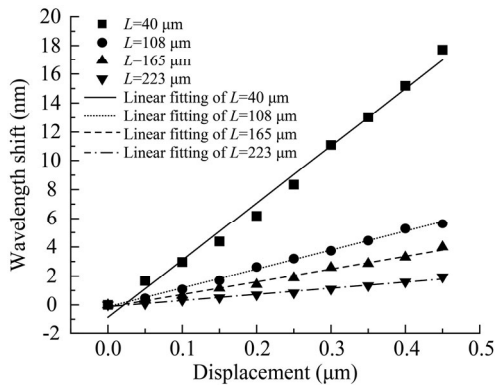
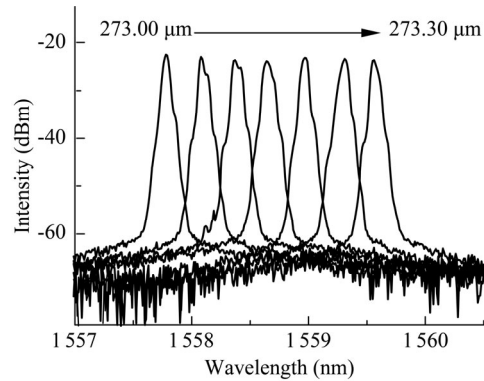


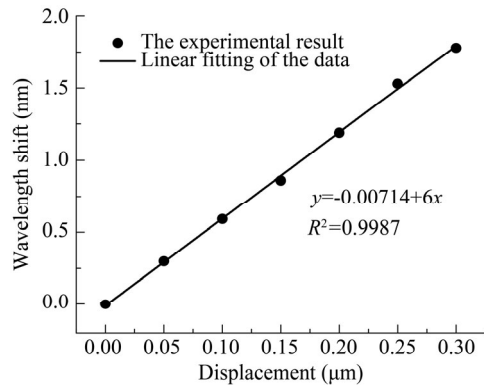
Fig.6 The wavelength shift as a function of the displacement with different original L values

Usually, the peak bandwidth of a laser is much narrower than that of a filter, and narrow bandwidth is easier to be distinguished by the detector. In addition, the bandwidth and the extinction ratio of a laser with certain filter are more beneficial than those only employing the filter. Therefore, the proposed FPI can act as the filter in the ring cavity fiber laser as shown in Fig.1. The length of the EDF (EDF1013, 6/125, YOFC) is about 10 m. The OSA (YOKOGAWA, AQ6375) is used to detect and record the spectra. The pump power is set as a constant of 200 mW. In the displacement sensing experiment

based on the fiber laser, the original L of $273\ \mu\text{m}$ is implemented. The wavelength of the peak moves to the long wavelength direction with the increase of displacement as shown in Fig.7(a). Moreover, the wavelength shift and the displacement present a good linear relationship, which can be obtained from Fig.7(b). The slope of the straight line in Fig.7(b) gives the sensitivity of $6\ \text{nm}/\mu\text{m}$ for micro-displacement sensing.



(a) The transmission spectra of the fiber laser with various displacements of $L=273.00\text{--}273.30\ \mu\text{m}$ with interval of $0.05\ \mu\text{m}$



(b) The wavelength shift with the increase of displacement

Fig.7 The experimental results of the FPI based ring cavity fiber laser for micro-displacement measurement

We propose and demonstrate a ring cavity fiber laser for micro-displacement sensing. The all fiber FPI is applied as the sensing component and the filter of the ring cavity fiber laser. The relationship between the transmission spectra of the FPI and the length of the FPC is investigated in both numerical simulation and experiment. It can be obtained that the wavelength corresponding to the peak moves to the long wavelength direction with the increase of the displacement. In addition, the experimental results show that the maximum sensitivity of the FPI is $39.6\ \text{nm}/\mu\text{m}$ with the original L of $40\ \mu\text{m}$, and the fiber laser provides a linear sensitivity of $6\ \text{nm}/\mu\text{m}$.

References

[1] Y. Zhu, P. Shum, C. Lu, M. B. Lacquet, P. L. Swart, A.

- A. Chtcherbakov and S. J. Spammer, *Optics Express* **11**, 1918 (2003).
- [2] A. S. Guru Prasad and S. Asokan, Fiber Bragg Grating Sensor Package for Submicron Level Displacement Measurements, *Experimental Techniques*, 1 (2013).
- [3] Z. Weigang, D. Xiaoyi, Z. Qida, G. Kai and Y. Shuzhong, *IEEE Photonics Technology Letters* **13**, 1340 (2001).
- [4] J. H. Ng, X. Zhou, X. Yang and J. Hao, *Optics Communications* **273**, 398 (2007).
- [5] H.-H. Zhu, J.-H. Yin, L. Zhang, W. Jin and J.-H. Dong, *Advances in Structural Engineering* **13**, 249 (2010).
- [6] J. Qi and H. Debo, *IEEE Sensors Journal* **11**, 1776 (2011).
- [7] X. Wen, T. Ning, H. You, Z. Kang, J. Li, C. Li, T. Feng, S. Yu and W. Jian, *Chinese Physics Letters* **31**, 034203 (2014).
- [8] C. Jinping, Z. Jun and J. Zhenhong, *IEEE Photonics Technology Letters* **25**, 2354 (2013).
- [9] F. Xie, J. Ren, Z. Chen and Q. Feng, *Optics & Laser Technology* **42**, 208 (2010).
- [10] Q. Rong, X. Qiao, Y. Du, D. Feng, R. Wang, Y. Ma, H. Sun, M. Hu and Z. Feng, *Applied Optics* **52**, 1441 (2013).
- [11] M. Bravo, A. M. R. Pinto, M. Lopez-Amo, J. Kobelke and K. Schuster, *Optics Letters* **37**, 202 (2012).
- [12] N. Ushakov and L. Liokumovich, *Applied Optics* **53**, 5092 (2014).
- [13] D. Jauregui-Vazquez, J. M. Estudillo-Ayala, A. Castillo-Guzman, R. Rojas-Laguna, R. Selvas-Aguilar, E. Vargas-Rodriguez, J. M. Sierra-Hernandez, V. Guzman-Ramos and A. Flores-Balderas, *Optics Communications* **308**, 289 (2013).
- [14] J. Chen, J. Zhou and X. Yuan, *IEEE Photonics Technology Letters* **26**, 837 (2014).
- [15] WEN Xiao-dong, NING Ti-gang, YOU Hai-dong, LI Jing, FENG Ting, PEI Li and JIAN Wei, *Optoelectronics Letters* **9**, 325 (2013).
- [16] Z. Tian, Yam S. S. H., Barnes J., Bock W., Greig P., Fraser J. M., Looock H. and Oleschuk R. D., *IEEE Photonics Technology Letters* **20**, 626 (2008).
- [17] CAO Ye, LIU Ce and TONG Zheng-rong, *Optoelectronics Letters* **10**, 401 (2014).